microPublication BIOLOGY

7/2/2026 - *Open Access*

BacQuant: A Scalable Automated Image Processing Pipeline for Quantifying Biofilm Aggregates

Tevin Flom[1,2], Umur A. Ciftci[1], Caitlin J. Light[1], Whitni K. Redman[1§]

[1]First-year Research Immersion Program, Binghamton University

[2]Department of Biological Sciences, Binghamton University

[§]To whom correspondence should be addressed: wredman@binghamton.edu

Abstract

Traditional microbiology methods rely on viable plate counting to quantify bacterial populations but often underestimate biofilm cell density because matrix-encased aggregates can produce a single colony despite containing many cells. Here, we present BacQuant, a computer vision pipeline developed in Python and OpenCV to quantify biofilm aggregates from brightfield microscopy images. Using image thresholding, segmentation, and contour detection, BacQuant distinguishes individual cells from aggregates and estimates total cell burden more comprehensively than viable plate counting alone. Automated counts closely matched manual microscopy counts while producing higher estimated densities, highlighting BacQuant as a scalable, inexpensive complimentary method for biofilm quantification.

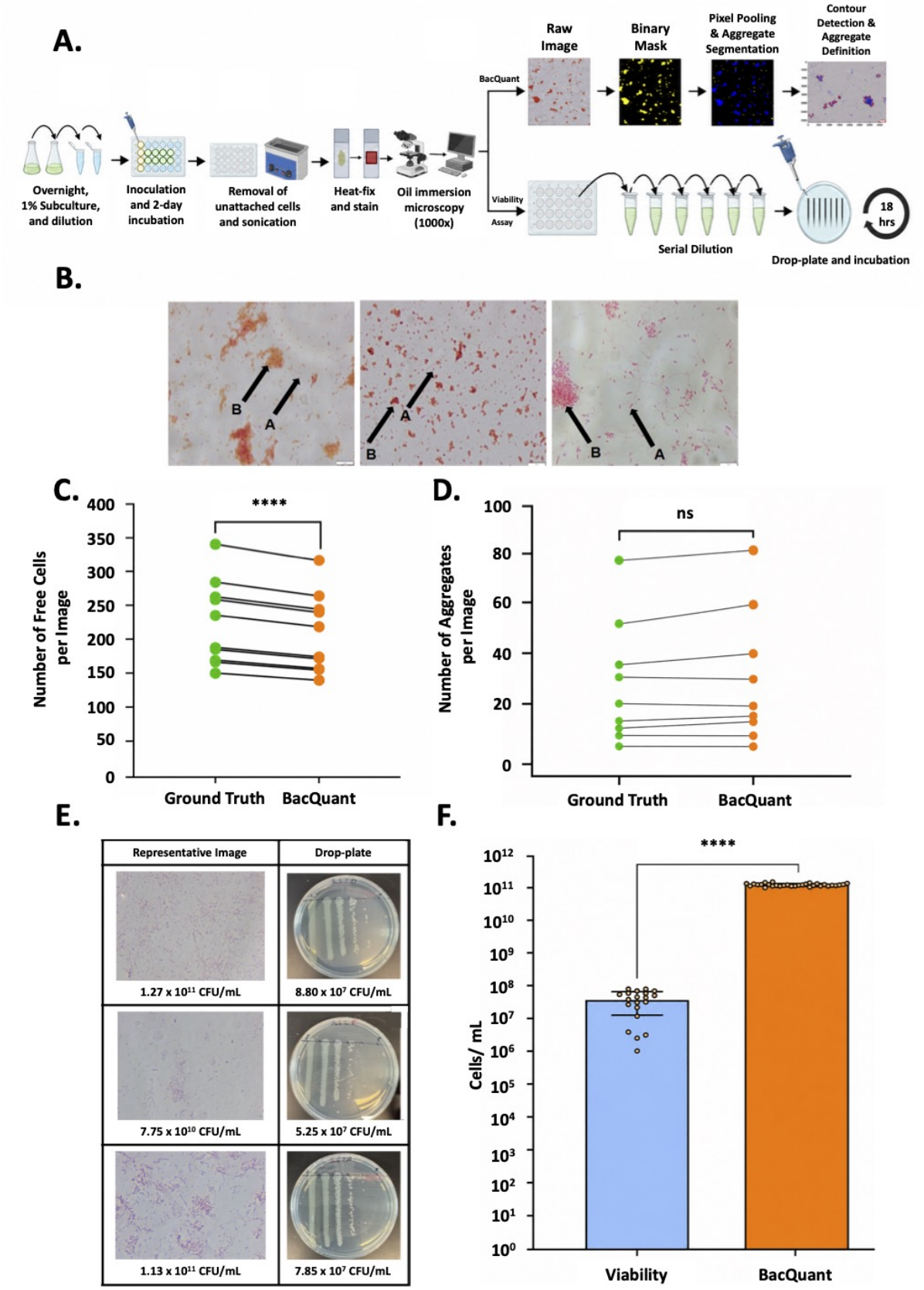

Figure 1. Work Flow and Representative Results of BacQuant:

(A) Biofilm growth, sample preparation, and analysis. 48-hour PAO1 biofilms were collected, rinsed to removed unattached cells, and sonicated to liberate biofilm-encased bacteria. The resulting suspension were mounted on slides, stained with safranin, and imaged by brightfield microscopy. Images were analyzed using the BacQuant pipeline to distinguish free cells from aggregates and determine cell counts. In parallel, cell viability was assessed by serial dilution

and plating to obtain CFU/mL measurements. **(B) Representative images of stained cell populations.** Cells were stained with a safranin-based counterstain for one minute in order to show both free cell and aggregate morphologies. Examples of free cells (A) and aggregates (B) are shown by the labeled arrows. These images were typical of the aforementioned experimental design. Representative of n= 32 images. Scale bars represent 10 µm. **(C,D) Validation of the Pipeline Against Ground-Truth Labels.** Estimation plots of free cells **(C)** and aggregates **(D)** are shown. Ground truth counts were obtained by manually counting the number of free cells and aggregates in each image. The ground truth counts across 10 representative images from the total experimental set of 300 images were measured, and the pipeline was run once on each sample image. The green circles represent ground truth counts, and orange circles represent BacQuant measurements. **(E,F) Comparison of BacQuant Against Viable Plate Cell Counts.** Viable plate counts were determined via serial dilution and drop-plating of the post-sonicated sample. Representative images of drop-plates and corresponding microscopy images **(E)**, along with the CFU/mL calculated from BacQuant (left column) and viable plate count (right column). Average cells/mL counts from BacQuant (orange bar) were compared against CFU/mL counts from viable plate counts (blue) in **(F)**. The estimation plots above were generated from paired t-tests.; ****, $p<0.0001$, n=10. Statistical significance was determined with an unpaired t-test, and error bars represent standard deviation. ****, $p<0.0001$, n=18-22 biofilm samples with 10 images per sample.

Description

Biofilms are communities of bacteria encased in a matrix composed of extracellular polymeric substances (EPS) including lipids, proteins, extracellular DNA, and polysaccharides (Flemming et al., 2025). These communities are ubiquitous across medical, industrial, and environmental systems and are responsible for an estimated $4 trillion in global economic damage annually (Camara et al., 2022). Clinically, biofilms contribute to approximately 80% of human infections, where the EPS confers protection from antibiotics and host immune responses (Fedorowski, Moller, & Melander, 2013). Both Gram-positive species, such as *Staphylococcus aureus*, and Gram-negative species, such as *Pseudomonas aeruginosa*, exhibit biofilm-associated tolerance and persistence that complicate treatment (Schaber et al., 2007; Usui, Yoshii, Thiriet-Rupert, Ghigo, & Beloin, 2023).

A major challenge in biofilm research is accurate quantification of bacterial populations following experimental treatment. Conventional colony-forming unit (CFU) or viable plate counting (VPC) methods remain widely used because they specifically measure culturable, viable bacteria. However, in biofilm samples, VPC may not fully reflect the total number of cells present because aggregates containing multiple cells can produce a single colony if they are not completely freed from the matrix before plating (Beal et al., 2020; Martini, Boddu, Nemenman, & Vega, 2024). Mechanical disruption methods, such as homogenization or sonication, are commonly used to break up biofilms prior to plating. While optimized detachment and sonication protocols can substantially improve biofilm separation, incomplete dissociation of EPS-bound aggregates may still occur depending on the organism, biofilm structure, treatments, and disruption protocol used (Buckingham-Meyer et al., 2022; Korshoj & Kielian, 2024).

Recent advances in computer vision and microscopy offer alternative strategies for microbial quantification. Image-based methods can distinguish individual cells from aggregates using segmentation and contour detection, providing structural information that is lost in culture-based approaches (Holicheva et al., 2025; J. Wang et al., 2022). However, existing tools such as BiofilmQ and confocal-based pipelines are computationally intensive, require specialized hardware, or are not designed for post-disruption enumeration (Hartmann et al., 2021; Mountcastle et al., 2021).

Here, we present BacQuant, a computationally inexpensive image processing pipeline to improve quantification of biofilm cells following sonication using brightfield microscopy. Using *P. aeruginosa* as a model organism, BacQuant differentiates free cells from aggregates and estimates aggregate cell numbers to improve quantification relative to VPC methods **(Figure 1A).** It is important to note that BacQuant does not intend to count viable cells. Rather, it estimates the total cell count in the biofilm sample including both live and dead cells. It does not estimate live cells like traditional VPC methods do.

Sonication of *P. aeruginosa* biofilms consistently yields two morphologies – free individual cells and EPS-encased aggregates (**Figure 1B**). Operationally, BacQuant defines these categories by segmented object size rather than by visual interpretation alone. Free cells displayed relatively uniform size and shape, whereas aggregates varied widely in morphology, often appearing circular with irregular edges and measuring up to ~1000 µm in diameter. Safranin staining revealed higher color saturation in aggregates, reflecting increased biomass and EPS. Both morphologies were present in all samples, indicating incomplete disaggregation by sonication.

To evaluate BacQuant performance, images were treated as biological replicates and manually annotated to generate ground truth labels. There was a significant difference ($p=0.0001$; **Figure 1C**) in the number of free cells identified by ground truth and those identified by BacQuant. This underestimation likely arises from pixel-based normalization to a user-defined average cell area, which does not account for cell orientation or morphological variability.

In contrast, BacQuant slightly overestimated aggregate counts compared to ground truth, although this difference was not statistically significant ($p=0.0569$; **Figure 1D**). This trend likely reflects conservative edge detection during segmentation

and the lack of depth information in two-dimensional images, which may obscure internal aggregate structure.

BacQuant total cell counts were compared to traditional VPC measurements obtained via serial dilution and drop-plating (**Figure 1A,E).** Across twenty samples, BacQuant produced significantly higher mean cell counts than VPC (p=0.0001), with averages of 1.18 x 10^{11} and 4.46 x 10^{7} cells, respectively (**Figure 1F**). BacQuant results were more tightly clustered, whereas VPC values exhibited greater variability.

This discrepancy is consistent with the presence of biofilm aggregates that contain many cells but yield only a single colony on agar plates. Additionally, BacQuant includes dead cells in its estimates, whereas VPC counts only viable cells, further contributing to higher total counts.

This study introduces BacQuant, a computationally inexpensive image-processing pipeline for quantifying biofilm cells following sonication. BacQuant addresses a fundamental limitation of CFU-based methods by explicitly accounting for residual aggregates that persist after mechanical disruption and confound viable cell estimates (Fleming et al., 2020). By combining thresholding with edge and contour detection, BacQuant enables reproducible instant segmentation of individual cells and aggregates.

Sonication was selected as the representative disruption method due to its widespread use in laboratory, clinical, and industrial contexts. While sonication effectively detaches biofilms from surfaces, it does not reliably dissociate biofilms into single cells, leaving EPS-bound aggregates intact (Kragh et al., 2016) (**Figure 1B**). These aggregates are indistinguishable from single cells in VPC assays, leading to systematic underestimation of bacterial load. BacQuant circumvents this issue by estimating the number of cells within aggregates, producing significantly higher and more consistent counts than VPC (**Figure 1F**).

A major strength of BacQuant is its accessibility. Unlike machine learning-based or confocal approaches, the pipeline does not require training data, specialized hardware, or bulky software installations. It can be run on standard CPUs and adapted to diverse imaging conditions, making it broadly applicable across laboratories. The method captures biologically meaningful structure features, specifically the distinction between free cells and aggregates, that are routinely missed by culture-based techniques.

Nevertheless, BacQuant has limitations. In dense images, over-segmentation may occur, leading to slight overestimation of aggregate numbers (**Figure 1D)**. Conversely, free cells are underestimated due to reliance on an average cell area parameter that does not account for morphological variability (**Figure 1C).** The pipeline also cannot distinguish between live and dead cells, which may inflate estimates relative to viable counts. If cells occur in small clusters like doublets or triplets, it is processed as an aggregate while they could be a few individual cells in close promixity to one another. Another major limitation is the imposition of 2D structure on the 3D aggregate morphology. Because BacQuant only uses two-dimensional estimation, edge detection is conservative and does not take the height of the structure into account when determining cell density within large cell clusters, dampening the true estimate of cell density within. Additionally, accurate performance depends on high-contrast microscopy images and correct calibration for each experimental setup.

Despite these constraints, BacQuant provides a rapid and scalable complement to traditional microbiological methods. The entire analysis can be completed within minutes, compared to hours or days required for plating assays. Accurate biofilm quantification is critical for antimicrobial testing, clinical research, and environmental monitoring, and BacQuant offers a practical tool for improving structural enumeration of bacterial populations (Folliero et al., 2021).

Future work should integrate live/dead staining, molecular viability markers, and three-dimension imaging to refine estimates of active biofilm populations (Sauer et al., 2022; Wang, Zhu, Zheng, Dong, & Liu, 2022). Incorporation of machine learning-based segmentation could further enhance classification of complex morphologies. Ultimately, BacQuant provides a foundation for automated, image-based biofilm quantification and highlights the value of computer vision approaches in microbiology research..

Methods

Materials and Methods

Bacterial Culture Preparation

P. aeruginosa PAO1 liquid cultures were routinely grown in lysogeny broth (LB) (SigmaAldrich®, Cat# L3022) at 37°C under 220 RPM shaking conditions for 18 hours in 125 mL flasks.

In vitro Well-plate Model

P. aeruginosa biofilms were cultivated in 24-well non-tissue culture-treated plates (VWR, Cat# 10861-558) for 48 hours at 37°C under 80 RPM shaking conditions. Individual wells were inoculated with 10^{6} CFU/mL in 800 µL. After the 48-hour incubation, media was removed, and each well was rinsed with 1 mL of 0.85% saline solution to remove any unattached

or lysed cells. This growth protocol was adapted from Fleming et. al (Fleming et al., 2020). The entire plate was covered with parafilm and placed into a water bath sonicator (Fischer Scientific, Cat# 15337411) for 30 minutes. This sonication condition was selected based on previously published biofilm disruption protocols (Fleming, Chahin, & Rumbaugh, 2017; Redman et al., 2021) and was not used independently optimized in the present study. Because the purpose of this work was to evaluate BacQuant as an image-based method for quantifying cells and residual aggregates following a standard disruption step, additional optimization of sonication intensity, during, or enzymatic pretreatment was outside the scope of this study. After sonication, the contents of each well were moved to a respective 1.5 mL microcentrifuge tube.

Slide Preparation and Viability Assay

After harvesting, 10 µL of cell solution was added onto a glass microscope slide (Globe Scientific, Inc, Cat# 1304). The solution was spread into a 1 cm^2 area at the center of each slide using an inoculation loop. The samples were then heat-fixed onto the slides and stained with Safranin Advanced Counterstain (Hardy Diagnostics, Cat# GK400) for 1 minute and subsequently rinsed with deionized water. The slides were then wet-mounted using immersion oil and topped with a glass cover slip. Concurrently, the remaining cell solution was serially diluted in saline and drop-plated onto solid LB agar and incubated for 18-24 hours at 37°C for CFU enumeration.

Brightfield Microscopy

All slides were imaged using an Olympus BX43 microscope under oil immersion at 100x magnification. Five representative images of each slide were taken, representing one well in the 24-well plate model. An Olympus DP22 camera was used with CellSens Entry software to take the images. The size of each image and light intensity was constant across all images. The dimensions of each image were measured to be 5000 x 7000 nm, in metric units using the Linear Ruler tool in CellSens Entry. Images were saved and label-matched to their corresponding drop-plate.

Image Analysis

A custom computer vision image analysis pipeline was built using Python v3.8 programming language. A stand-alone version of the pipeline is provided and can be run as an online notebook in or as a script with a Python IDE. All necessary interaction with the code is clearly labeled for the user as comments in the code, as this pipeline is not based on a graphical user interface (GUI). This pipeline should be adapted for individual experiments, as it is currently optimized for use with *P. aeruginosa* mono-species biofilm cells. All parameters are clearly labeled in the code and are easily customizable. All code is freely available, with the implementation of each step of the pipeline clearly shown. The code is available through Google Colaboratory (https://colab.research.google.com/drive/1JWpmjoXKtgYmeux7MUyBH6syZLHm1inf?usp=sharing). We recommend this pipeline be used with GPU acceleration for high-throughput analyses, but running the process in the cloud or with a CPU is also easily supported. The pipeline takes *.png* file format images as the primary input, as well as user-specified parameters such as the area of an individual cell in pixels and image size.

The first step of the pipeline entails generating a binary mask of the image based on color threshold values. The mask eliminates background noise in the image and standardizes the shape and sizes of all image features. Following masking, a diameter-based size thresholding algorithm is used to label large connected regions in the image as aggregates in blue, and smaller regions as free cells in yellow. This simplifies the visual distinction between aggregates and free cells. From this color-changing step, the percentages of aggregated biomass and free cells are determined via color-based pixel pooling. For the purpose of this analysis, an aggregate is defined as any connected segmented region with an estimated diameter greater than the user-defined threshold for a single cell. Segmented regions at or below this threshold are classified as free cells. Smaller clusters like doublets, triplets, and quadruplets are classified according to the same size-based rules and were not assigned separate biological categories. If the connected region exceeds the aggregate threshold, it is labeled as an aggregate and its cell number is estimated by dividing the segmented area by the user defined single-cell average area in pixels. If the region does not exceed the threshold, it is classified as a free-cell region.

Concurrently, a contour detection algorithm from the OpenCV (https://github.com/itseez/opencv) library is used to extract aggregated regions of cells as features. The edges of each aggregate are separated from the background image using Canny edge detection (DOI: 10.1109/TPAMI.1986.4767851). Then, the remaining regions are enclosed by a boundary line through contour detection. This allows for the thorough definition of the 2D shape of each aggregate. From these contours, the area of each aggregate is calculated in pixels and converted to square microns. Cell counts within the aggregates are based on the area of an individual cell in pixels, which is defined by the user at the beginning of the pipeline. It is important to note that this process only works on two-dimensional images. It also can be used with epifluorescence

microscopy and live/dead staining with modification in the image processing code to exclude dead cells. It is not optimized for Z-stack images, though it can be modified to work with image arrays and high-throughput imaging results. This makes BacQuant a useful tool for more basic laboratories without complex equipment, software, or imaging capabilities.

The output of this pipeline includes the percent aggregated biomass in each image, number of aggregates, estimated number of cells in aggregates, total estimated cells in each image, and estimated calculation of cells per mL of solution. The raw data from this analysis is stored as a *.csv* file format spreadsheet. We recommend that further processing of the data be conducted in Microsoft Excel.

Statistical Analysis

Statistical analysis was conducted using GraphPad Prism. A paired t-test was utilized to compare ground truth and BacQuant counts of aggregates and free cells. An unpaired t-test was used to compare viable plate count assay results with BacQuant results. All analyses were conducted to determine statistical significance with an alpha value of 0.05.

References

Acosta N, Waddell B, Heirali A, Somayaji R, Surette MG, Workentine ML, Rabin HR, Parkins MD. 2020. Cystic Fibrosis Patients Infected With Epidemic Pseudomonas aeruginosa Strains Have Unique Microbial Communities. Frontiers in Cellular and Infection Microbiology 10: 10.3389/fcimb.2020.00173. DOI: 10.3389/fcimb.2020.00173

Beal J, Farny NG, Haddock-Angelli T, Selvarajah V, Baldwin GS, Buckley-Taylor R, et al., Zhou. 2020. Robust estimation of bacterial cell count from optical density. Communications Biology 3: 10.1038/s42003-020-01127-5. DOI: 10.1038/s42003-020-01127-5

Bjerkan G, Witsø E, Bergh Kr. 2009. Sonication is superior to scraping for retrieval of bacteria in biofilm on titanium and steel surfaces in vitro. Acta Orthopaedica 80: 245-250. DOI: 10.3109/17453670902947457

Buckingham-Meyer K, Miller LA, Parker AE, Walker DK, Sturman P, Novak I, Goeres DM. 2022. Harvesting and Disaggregation: An Overlooked Step in Biofilm Methods Research. Journal of Visualized Experiments : 10.3791/62390. DOI: 10.3791/62390

Cámara M, Green W, MacPhee CE, Rakowska PD, Raval R, Richardson MC, et al., Webb. 2022. Economic significance of biofilms: a multidisciplinary and cross-sectoral challenge. npj Biofilms and Microbiomes 8: 10.1038/s41522-022-00306-y. DOI: 10.1038/s41522-022-00306-y

Fedorowski A, Möller SJ, Melander O. 2013. Response to the letter by prof. Dal Moro: the Dark Side of the Swoon–antihypertensive treatment in the elderly. Journal of Internal Medicine 274: 293-294. DOI: 10.1111/joim.12086

Fleming D, Chahin L, Rumbaugh K. 2017. Glycoside Hydrolases Degrade Polymicrobial Bacterial Biofilms in Wounds. Antimicrobial Agents and Chemotherapy 61: 10.1128/aac.01998-16. PubMed ID: 27872074

Fleming D, Redman W, Welch GS, Mdluli NV, Rouchon CN, Frank KL, Rumbaugh KP. 2020. Utilizing glycoside hydrolases to improve the quantitation and visualization of biofilm bacteria. Biofilm 2: 100037. DOI: 10.1016/j.bioflm.2020.100037

Flemming HC, van Hullebusch ED, Little BJ, Neu TR, Nielsen PH, Seviour T, et al., Wuertz. 2024. Microbial extracellular polymeric substances in the environment, technology and medicine. Nature Reviews Microbiology 23: 87-105. DOI: 10.1038/s41579-024-01098-y

Folliero V, Franci G, Dell'Annunziata F, Giugliano R, Foglia F, Sperlongano R, et al., Galdiero. 2021. Evaluation of Antibiotic Resistance and Biofilm Production among Clinical Strain Isolated from Medical Devices. International Journal of Microbiology 2021: 1-11. DOI: 10.1155/2021/9033278

Fowler TE, Bloomquist RF, Sakhalkar MV, Bloomquist DT. 2023. Chronic Purulent Conjunctivitis Associated With Extensively Drug-Resistant *Pseudomonas aeruginosa*. JAMA Ophthalmology 141: 609. DOI: 10.1001/jamaophthalmol.2023.1529

Goldufsky J, Wood SJ, Jayaraman V, Majdobeh O, Chen L, Qin S, et al., Shafikhani. 2015. *Pseudomonas aeruginosa* uses T3SS to inhibit diabetic wound healing. Wound Repair and Regeneration 23: 557-564. DOI: 10.1111/wrr.12310

Gonzalez MR, Fleuchot B, Lauciello L, Jafari P, Applegate LA, Raffoul W, Que YA, Perron K. 2016. Effect of Human Burn Wound Exudate on Pseudomonas aeruginosa Virulence. mSphere 1: 10.1128/msphere.00111-15. DOI: 10.1128/mSphere.00111-15

Hartmann R, Jeckel H, Jelli E, Singh PK, Vaidya S, Bayer M, et al., Drescher. 2021. Quantitative image analysis of microbial communities with BiofilmQ. Nature Microbiology 6: 151-156. DOI: 10.1038/s41564-020-00817-4

Holicheva AA, Kozlov KS, Boiko DA, Kamanin MS, Provotorova DV, Kolomoets NI, Ananikov VP. 2025. Deep generative modeling of annotated bacterial biofilm images. npj Biofilms and Microbiomes 11: 10.1038/s41522-025-00647-4. DOI: 10.1038/s41522-025-00647-4

Klinger-Strobel M, Suesse H, Fischer D, Pletz MW, Makarewicz O. 2016. A Novel Computerized Cell Count Algorithm for Biofilm Analysis. PLOS ONE 11: e0154937. DOI: 10.1371/journal.pone.0154937

Korshoj LE, Kielian T. 2024. Bacterial single-cell RNA sequencing captures biofilm transcriptional heterogeneity and differential responses to immune pressure. bioRxiv: pii: 2024.06.28.601229. 10.1101/2024.06.28.601229. PubMed ID: 38979200

Kragh KN, Hutchison JB, Melaugh G, Rodesney C, Roberts AEL, Irie Y, et al., Bjarnsholt. 2016. Role of Multicellular Aggregates in Biofilm Formation. mBio 7: 10.1128/mbio.00237-16. DOI: 10.1128/mBio.00237-16

Martini KM, Boddu SS, Nemenman I, Vega NM. 2024. Maximum likelihood estimators for colony-forming units. Microbiology Spectrum 12: 10.1128/spectrum.03946-23. DOI: 10.1128/spectrum.03946-23

Mountcastle SE, Vyas N, Villapun VM, Cox SC, Jabbari S, Sammons RL, et al., Kuehne. 2021. Biofilm viability checker: An open-source tool for automated biofilm viability analysis from confocal microscopy images. npj Biofilms and Microbiomes 7: 10.1038/s41522-021-00214-7. DOI: 10.1038/s41522-021-00214-7

Redman WK, Welch GS, Williams AC, Damron AJ, Northcut WO, Rumbaugh KP. 2021. Efficacy and safety of biofilm dispersal by glycoside hydrolases in wounds. Biofilm 3: 100061. PubMed ID: 34825176

Sauer K, Stoodley P, Goeres DM, Hall-Stoodley L, Burmølle M, Stewart PS, Bjarnsholt T. 2022. The biofilm life cycle: expanding the conceptual model of biofilm formation. Nature Reviews Microbiology 20: 608-620. DOI: 10.1038/s41579-022-00767-0

Schaber JA, Triffo WJ, Suh SJ, Oliver JW, Hastert MC, Griswold JA, et al., Rumbaugh. 2007. *Pseudomonas aeruginosa* Forms Biofilms in Acute Infection Independent of Cell-to-Cell Signaling. Infection and Immunity 75: 3715-3721. DOI: 10.1128/IAI.00586-07

Stoodley P, Sauer K, Davies DG, Costerton JW. 2002. Biofilms as Complex Differentiated Communities. Annual Review of Microbiology 56: 187-209. DOI: 10.1146/annurev.micro.56.012302.160705

Usui M, Yoshii Y, Thiriet-Rupert S, Ghigo JM, Beloin C. 2023. Intermittent antibiotic treatment of bacterial biofilms favors the rapid evolution of resistance. Communications Biology 6: 10.1038/s42003-023-04601-y. DOI: 10.1038/s42003-023-04601-y

Wang J, Tabassum N, Toma TT, Wang Y, Gahlmann A, Acton ST. 2022. 3D GAN image synthesis and dataset quality assessment for bacterial biofilm. Bioinformatics 38: 4598-4604. DOI: 10.1093/bioinformatics/btac529

Wang S, Zhu H, Zheng G, Dong F, Liu C. 2022. Dynamic Changes in Biofilm Structures under Dynamic Flow Conditions. Applied and Environmental Microbiology 88: 10.1128/aem.01072-22. DOI: 10.1128/aem.01072-22

Funding: This work was supported by the First-year Research Immersion Program at Binghamton University, the Binghamton University Scholars Program, and the Harpur's Edge Award from the External Scholarship and Undergraduate Research Center at Binghamton University.

Conflicts of Interest: The authors declare that there are no conflicts of interest present.

Author Contributions: Tevin Flom: conceptualization, data curation, formal analysis, methodology, writing - original draft. Umur A. Ciftci: conceptualization, formal analysis, supervision, writing - review editing. Caitlin J. Light: conceptualization, methodology, resources, supervision, writing - review editing. Whitni K. Redman: conceptualization, formal analysis, funding acquisition, methodology, project administration, resources, supervision, writing - original draft, writing - review editing, validation.

Reviewed By: Ilana Kolodkin Gal

History: Received February 2, 2026 **Revision Received** May 22, 2026 **Accepted** June 24, 2026 **Published Online** July 2, 2026 **Indexed** July 16, 2026

Citation: Flom T, Ciftci UA, Light CJ, Redman WK. 2026. BacQuant: A Scalable Automated Image Processing Pipeline for Quantifying Biofilm Aggregates. microPublication Biology. 10.17912/micropub.biology.002045